

The mafic mineralogy of the peralkaline syenites and granites of the Mulanje complex, Malawi

R. GARTH PLATT

Department of Geology, Lakehead University, Thunder Bay, Ontario, Canada

AND

ALAN R. WOOLLEY

Department of Mineralogy, British Museum (Natural History), London, England

ABSTRACT. Studies of the mafic mineralogy of the Mulanje granite-quartz-syenite-syenite Massif of southern Malawi delineate two mineralogically distinct complexes—the Main complex and the Chambe complex. Each complex is associated with its own trend of pyroxene evolution. The Main complex pyroxenes exhibit initial enrichment in hedenbergite before subsequent enrichment in acmite (i.e. sodic-salite-sodic-hedenbergite-aegirine-hedenbergite-aegirine), whereas the Chambe pyroxenes display constantly increasing acmite content with no significant enrichment in hedenbergite (i.e. sodic-salite-aegirine-augite-aegirine). This phenomenon is also reflected in the more Mg-rich amphiboles and biotites of the Chambe rocks when compared to those of the Main complex.

The general evolutionary trend of the Main complex amphiboles is katophorite → ferrorichterite → arfvedsonite which broadly correlates with a change in rock type from syenite to granite. Superimposed on this trend is an essentially similar, yet less extensive trend of the more Mg-rich Chambe amphiboles. The micas of both complexes show a general evolution to more iron-rich compositions with relatively constant Al content. Those of the Main complex, however, display extreme iron enrichment with ultimate formation of essentially pure ferrous annite.

Aenigmatite, astrophyllite, fayalite, chevkinite, yttrifluorite, and unidentified RE minerals are characteristic of the Main complex rocks but totally absent from those of the Chambe complex. Ilmenite constitutes the only iron oxide phase in the Main complex rocks whereas titaniferous magnetite (now unmixed) and ilmenite are both present in the rocks of Chambe.

The differences between the two complexes are explained in terms of oxygen fugacity, silica activity, crystallization interval, and the relative rates of development of peralkalinity. In essence, the Chambe magmas are considered to have crystallized under high f_{O_2} conditions with an earlier development of peralkaline tendencies when compared to those of the Main complex magmas. Moreover, a lower initial silica activity, a smaller alkali to alumina ratio, and a correspondingly smaller crystalliza-

tion interval could account for the lack of highly evolved granitic magmas in the Chambe complex, whereas such magmas are integral in the evolution of the Main complex.

KEYWORDS: mafic minerals, peralkaline syenites, granites, Mulanje complex, Malawi.

THE Upper Jurassic to Cretaceous igneous intrusions that lie in southern Malawi and adjacent parts of Mozambique form the Chilwa Alkaline Province. A review of the magmatism, age, and tectonic setting of this province is to be found in Woolley and Garson (1970). The intrusions vary widely in composition and include carbonatites, with or without associated nepheline syenite and nephelinite/ijolite, complexes of syenite and nepheline syenite, and silica-saturated to oversaturated complexes of syenite, quartz syenite, and granite.

The largest of the silica-saturated to oversaturated complexes is the Mulanje Massif, which rises steeply from the Palombe Plain to an altitude of some 3000 m, situated approximately 50 km east of Blantyre. The massif covers an area of 640 km² and consists of a series of coalescing syenite, quartz syenite, and granite intrusions which intrude the Precambrian gneisses of the Mozambique Belt. Syenitization or fenitization of the country rocks for up to 1 km is observed locally, although other contacts are sharp with no alteration and some display a contact breccia zone.

A detailed account of the geology and petrography of Mulanje is given by Garson and Walshaw (1969). This paper provides the first detailed account of the mineralogy of the Mulanje rocks and in particular of the chemistry of the mafic minerals. It is a study based on material collected by the authors principally from the northern and western parts of the Massif (fig. 1). Considerable care was

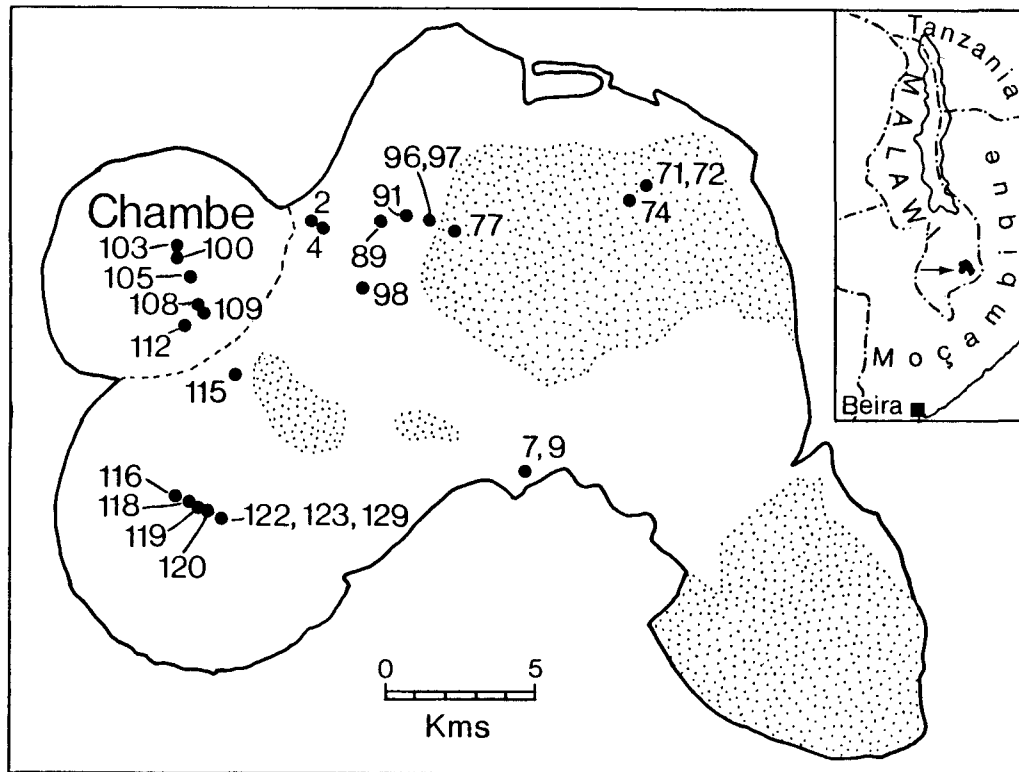


FIG. 1. Outline map of the Mulanje Massif indicating position of the Chambe complex and sources of specimens used in this study. Shaded areas indicate areas mapped as granite by Walshaw (in Garson and Walshaw, 1969).

taken to ensure that only reasonably unweathered material was collected, as bauxitization of the rocks is widespread. In general, the samples studied contain unaltered mafic minerals although the feldspars are invariably cloudy.

It will be shown here that the Mulanje Massif consists of two mineralogically distinct complexes, hereafter referred to as the Chambe complex and the Main complex. The Chambe complex, located on the NW side of the massif (fig. 1), was interpreted as a ring complex with a central plug by Stringer *et al.* (1956) on the basis of aerial photograph investigations, but Walshaw (in Garson and Walshaw, 1969) was unable to map individual rings in the field. Our work, however, supports the concept of a discrete Chambe complex.

Petrography

Detailed petrographic descriptions of the rocks of the Mulanje Massif are given by Walshaw (in Garson and Walshaw, 1969) and consequently only a brief account will be presented here.

The Main complex rocks vary from quartz-bearing syenites to granites. In general they contain more quartz than the Chambe complex rocks, which are essentially syenites and quartz syenites. Aenigmatite commonly occurs in the Main complex and astrophyllite, chevkinite, other unidentified RE minerals, and yttrifluorite are often present in the peralkaline granites of this complex. These phases are absent however from the rocks of the Chambe complex. Accessory sphene, zircon, and apatite are present in both complexes.

In both complexes, feldspar occurs as a single perthite phase sometimes rimmed by secondary albite/oligoclase. Brecciation and recrystallization of the feldspar is also observed. In general, the feldspar is anhedral although a few rocks, particularly from the Chambe complex, display aligned subhedral to euhedral prisms of feldspar which probably indicate a cumulus origin.

Pyroxene is common in both complexes, forming subhedral stubby prisms which are invariably partially replaced by amphibole. Pyroxene occurs as inclusions in feldspar and occasionally as inter-

sertal patches. Amphibole is ubiquitous and varies from green and brown sodic calcic varieties to deep blue sodic types. It is never euhedral and rarely forms substantial anhedral crystals. In general, the amphibole occurs either as intersertal patches and sub-poikilitic patches between and around feldspar or as replacements, most commonly rimming pyroxene. It occasionally forms aggregates with or without pyroxene, aenigmatite, biotite and an opaque phase. Textural evidence consistently indicates that pyroxene crystallized before amphibole. In only one sample has 'late' aegirine been observed rimming amphibole.

Tiny stellate clusters of blue amphibole, growing generally into quartz and occasionally into feldspar from more substantial amphiboles, are strongly reminiscent of textures seen in fenites. Tiny brown needles of similar habit are probably mica. These late-stage amphiboles and micas may represent a hydrothermal sub-solidus stage of crystallization.

Brown to reddish-brown biotite is not uncommon in rocks of both complexes, as is ilmenite. Titanomagnetite, now extensively unmineralized, is found only in rocks from the Chambe complex,

whereas fayalite, generally extensively altered, is only found in rocks from the Main complex.

Mineralogy

Of the more than 100 samples collected from the Chambe and Main complexes of Mulanje, 27 were chosen for detailed electron microprobe studies. The locations of these samples are given in fig. 1. Analyses were performed at the British Museum (Natural History) using a Cambridge Instruments Geoscan and Link Systems energy dispersive analyser with an acceleration voltage of 15 kV. During the study, particular attention was paid to the nature of the mafic and opaque minerals.

Clinopyroxenes. Representative analyses of clinopyroxenes from the Chambe and Main complexes of the Mulanje Massif are given in Table I and the full range of pyroxene analyses, in terms of diopside, hedenbergite, and acmite components is shown in fig. 2. Here, two distinct trends of pyroxene evolution are apparent, the Chambe complex trend and the Main complex trend.

TABLE I
REPRESENTATIVE ANALYSES OF PYROXENES

Sample	Main complex						Chambe complex		
	96	97	97	77	96	120	103	103	108
SiO ₂	50.69	49.81	49.72	50.19	51.09	52.65	53.15	51.52	52.05
Al ₂ O ₃	0.34	0.33	0.57	0.35	0.38	0.37	0.90	0.40	0.46
TiO ₂	0.48	0.29	0.41	0.22	0.85	1.31	0.50	0.50	0.31
Fe ₂ O ₃ *	3.78	5.91	6.97	12.31	17.23	28.94	5.64	14.17	21.65
FeO	16.47	14.85	15.60	15.00	12.17	3.33	5.42	11.19	7.69
MnO	1.30	1.27	1.23	1.27	0.72	0.37	1.42	1.18	0.88
MgO	6.98	5.32	4.01	1.33	0.61	0.05	12.72	2.52	1.38
CaO	19.98	18.30	18.37	13.64	9.63	1.51	20.33	11.43	6.83
Na ₂ O	1.13	2.32	2.65	5.22	7.68	12.26	1.84	6.64	9.23
ZrO ₂	0.04	0.00	0.00	0.22	0.14	0.04	0.17	0.44	0.13
Total	101.19	98.40	99.53	99.75	100.50	100.83	100.25	99.99	100.61
Structural formula based on 4 cations and 6 oxygens.									
Si	1.965	1.985	1.972	1.998	2.001	2.004	1.951	2.011	2.009
Al	0.016	0.015	0.027	0.016	0.018	0.017	0.039	0.018	0.020
Ti	0.014	0.009	0.012	0.007	0.025	0.037	0.013	0.015	0.008
Fe ^{3+*}	0.110	0.177	0.208	0.368	0.508	0.829	0.156	0.416	0.629
Fe ²⁺	0.534	0.495	0.518	0.499	0.399	0.106	0.166	0.365	0.248
Mn	0.043	0.043	0.041	0.043	0.023	0.012	0.044	0.039	0.029
Mg	0.403	0.316	0.237	0.079	0.036	0.003	0.696	0.147	0.079
Ca	0.830	0.781	0.781	0.582	0.404	0.062	0.800	0.478	0.282
Na	0.085	0.179	0.203	0.403	0.583	0.930	0.131	0.503	0.691
Zr	0.001	0.000	0.000	0.004	0.003	0.001	0.003	0.008	0.002
Molecular per cent of end-member molecules									
Di	38.0	30.3	23.9	7.8	3.5	0.3	67.3	14.3	6.9
Hd	54.2	51.8	56.4	53.2	40.7	7.0	20.3	39.2	24.1
Ac	7.8	17.9	19.7	39.0	55.8	92.7	12.4	46.5	69.0

Fe₂O₃* calculated on the basis of 4 cations and 6 oxygens.

Di=CaMgSi₂O₆; Hd=CaFe²⁺Si₂O₆; Ac=NaFe³⁺Si₂O₆. Proportions calculated after the method of Larsen (1976).

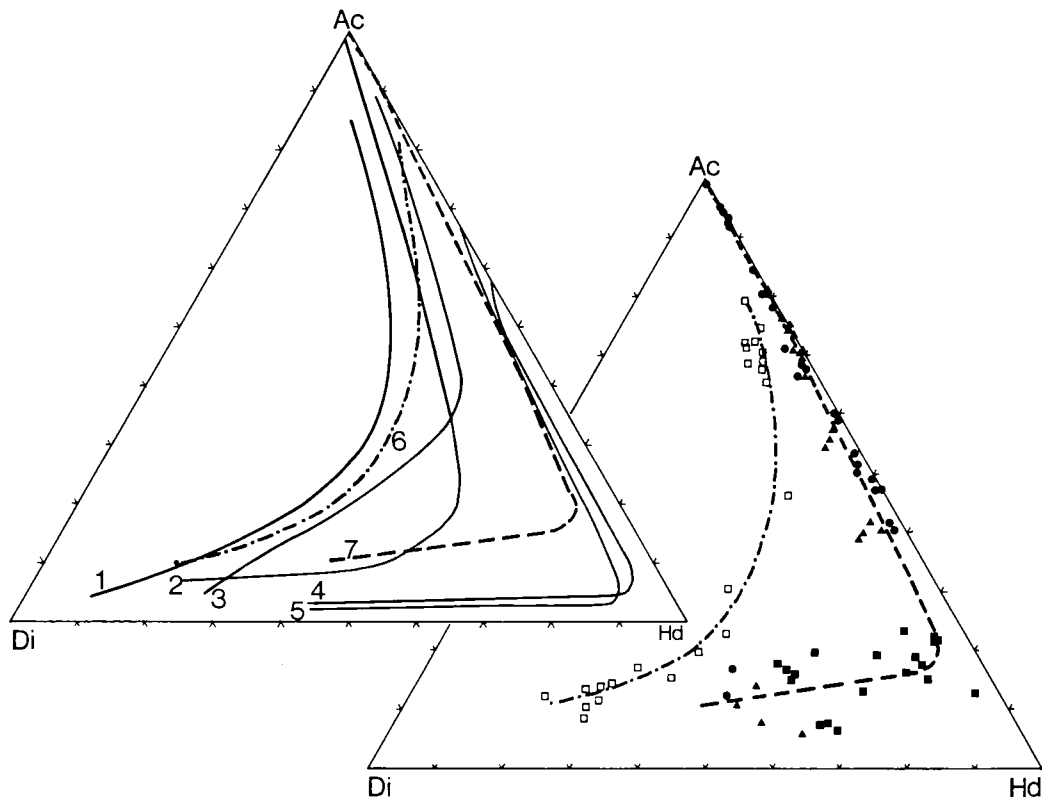


FIG. 2. *Right.* Overall trends of pyroxene compositions from the Mulanje Massif plotted in the system Di-Hd-Ac. *Left.* Additional trends for: 1, Uganda (Tyler and King, 1967); 2, South Qôroq (Stephenson, 1972); 3, Morotu, Sakhalin (Yagi, 1953); 4, Ilímaussaqa (Larsen, 1976); 5, Coldwell ferroaugite syenites (Mitchell and Platt, 1978). Trends 6 and 7 are those from the Chambe and Main complexes of Mulanje respectively. Open symbols, Chambe; solid symbols, Main complex.

The Chambe trend (sodic-salite-aegirine-augite aegirine) is characterized by constantly increasing acmite content with no significant enrichment in hedenbergite (maximum approximately 40 mol. %). Conversely, the Main pyroxene trend (sodic-ferrosalite-sodic-hedenbergite aegirine-hedenbergite aegirine) involves an initial enrichment in hedenbergite (maximum 80 mol. %) before subsequent enrichment in acmite. Thus, for a given acmite content, the Chambe pyroxenes are consistently more magnesian than those of the Main complex. This phenomenon is also reflected in the more Mg-rich amphiboles and biotites of the Chambe rocks when compared with those from the Main complex (see Tables II and III).

The explanation for these two trends must in part lie in differences between the chemistry of the parental magmas and in part in differences in the subsequent conditions of magmatic crystallization. Silica activity can be eliminated, however, as a

major cause of the differences. Both suites of rocks are silica-oversaturated and it has been consistently shown that both silica-undersaturated and oversaturated syenitic complexes display similar trends in pyroxene evolution (e.g. Larsen, 1976; Mitchell and Platt, 1978 and 1982; Neumann, 1976; Stephenson and Upton, 1982). Fugacity of oxygen (f_{O_2}) and peralkalinity of the evolving liquids may, however, play important roles in the subsequent trends of pyroxene evolution (Nash and Wilkinson, 1970; Larsen, 1976; Mitchell and Platt, 1978; Stephenson and Upton, 1982).

Although sodium enrichment of pyroxenes can occur under conditions of low f_{O_2} (Nash and Wilkinson, 1970; Mitchell and Platt, 1978), it is consistently observed that when f_{O_2} rises above the quartz-fayalite-magnetite (QFM) buffer sodium enrichment is enhanced with the ultimate generation of aegirine-rich pyroxenes (Nash and Wilkinson, 1970; Stephenson and Upton, 1982). There is

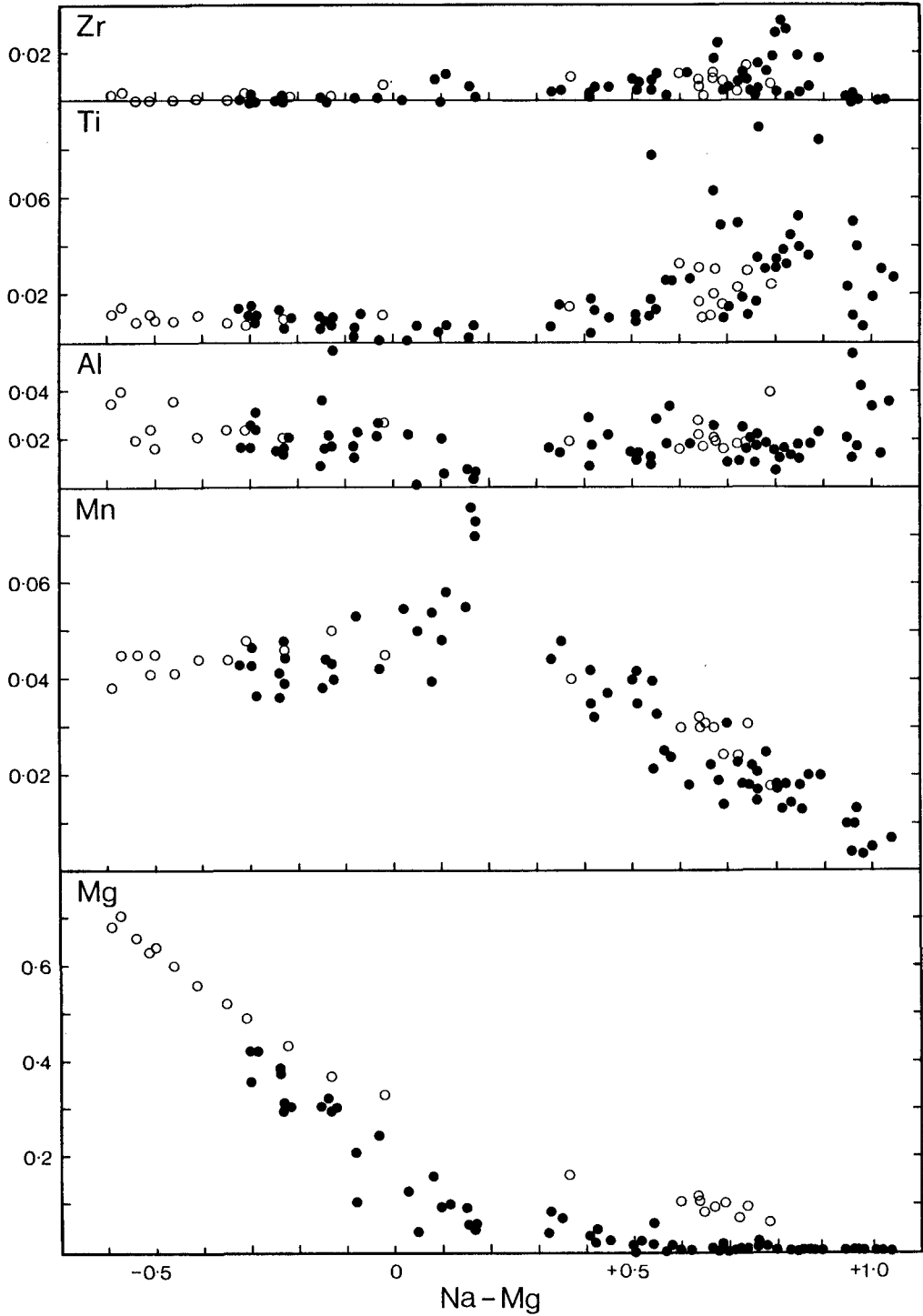
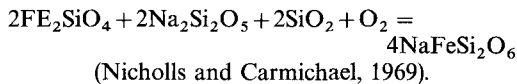


FIG. 3. Minor element trends of the Mulanje Massif pyroxenes plotted against (Na-Mg). Open symbols, Chambe; solid symbols, Main complex.

considerable evidence that the Chambe magmas were initially, and perhaps throughout their evolution, subject to higher f_{O_2} than those of the Main complex.

Fayalite is absent from the Chambe rocks but titanomagnetite (magnetite/ilmenite exsolution pairs) is a common accessory mineral. The f_{O_2} for these silica-oversaturated magmas is therefore above the QFM buffer. Moreover, primary sphene in the Chambe rocks also indicates an f_{O_2} above the QFM buffer (Carmichael and Nicholls, 1967), as does the absence of aenigmatite. Conversely, the presence of fayalite and the absence of titanomagnetite in rocks from the Main complex delineates an f_{O_2} below that of the QFM buffer. This is true, at least, for all but the most peralkaline magmas. Under these conditions, fayalite may cease to crystallize as a consequence of the reaction



Consequently, f_{O_2} may rise above that of the QFM buffer without the concomitant crystallization of magnetite.

Enhanced alkali contents of silicate liquids produces an increase in the Fe^{3+}/Fe^{2+} ratio (Paul and Douglas, 1965; Fudali, 1965). This is of fundamen-

tal concern in the generation of acmite-enriched pyroxenes. Increasing peralkalinity of liquids and the stage in evolution at which this occurs will be important influences on the actual trends of pyroxene compositions observed in a comagmatic suite of rocks. Early development of peralkalinity will cause a correspondingly early trend of acmite enrichment in the pyroxenes, while delay will allow greater enrichment of the hedenbergite molecule (see for example, Mitchell and Platt, 1978; Stephenson and Upton, 1982).

The degree of peralkalinity, the stage at which it first develops and the f_{O_2} of the liquids acting in concert will have a profound effect on the trend shown by pyroxenes in the Di-Hd-Ac diagram. It is proposed that the sodic-salite-aegirine-augite-aegirine trend exhibited by the Chambe pyroxenes (fig. 2) is a function of a higher f_{O_2} , perhaps associated with an earlier development of alkali-enriched liquids, when compared with those of the Main complex.

Pyroxenes of the two trends show no fundamental differences of minor element chemistry (fig. 3). Consequently, they will be discussed together. Zr and Ti become enriched in the more acmitic pyroxenes (fig. 3) although actual amounts are somewhat variable, even within pyroxenes from a single rock. This may result from the crystallization

TABLE II
REPRESENTATIVE ANALYSES OF AMPHIBOLES

Sample	Main complex							Chambe complex				
	116	91	9	98	120	122	115	100	105	103	112	109
SiO ₂	46.72	47.69	49.39	49.84	50.71	48.68	50.21	49.60	47.01	49.21	51.06	52.38
Al ₂ O ₃	2.72	1.58	1.29	0.50	0.55	1.58	0.56	2.46	3.85	3.62	1.21	0.50
TiO ₂	1.21	2.14	1.38	1.82	1.68	1.94	1.68	0.36	2.38	2.14	1.31	0.26
Fe ₂ O ₃	1.38	1.35	5.12	3.55	2.91	5.12	1.23	6.22	1.80	0.08	5.71	14.43
FeO	28.56	30.39	26.93	29.05	28.84	26.62	30.83	17.87	17.21	17.44	19.10	18.87
MnO	1.37	1.78	1.33	1.41	1.64	1.04	1.27	2.01	1.25	1.16	1.64	0.27
MgO	2.92	1.07	2.28	1.43	1.25	1.92	0.47	7.87	9.84	10.54	6.63	3.30
CaO	6.84	5.66	3.73	2.95	1.46	2.90	0.70	8.03	7.41	7.26	2.11	0.13
Na ₂ O	4.94	4.73	6.05	6.20	7.09	5.85	8.16	3.15	4.94	5.02	7.50	6.89
K ₂ O	1.01	1.12	1.17	1.78	2.17	1.87	1.70	1.10	1.20	1.34	1.49	0.17
Total	97.67	97.51	98.67	98.53	98.30	97.52	96.81	98.67	96.89	97.81	97.76	97.70
Structural formula based on 23 oxygens												
Si	7.473	7.683	7.751	7.893	8.022	7.731	8.096	7.513	7.206	7.402	7.809	8.045
Al	0.513	0.300	0.238	0.093	0.103	0.296	0.106	0.439	0.696	0.642	0.218	0.090
Ti	0.146	0.259	0.163	0.217	0.200	0.232	0.204	0.041	0.274	0.242	0.151	0.030
Fe ³⁺	0.166	0.164	0.604	0.423	0.346	0.612	0.150	0.709	0.207	0.009	0.657	1.652
Fe ²⁺	3.820	4.095	3.534	3.848	3.816	3.536	4.158	2.264	2.207	2.194	2.442	2.400
Mn	0.186	0.243	0.177	0.189	0.220	0.140	0.173	0.258	0.162	0.148	0.212	0.035
Mg	0.696	0.257	0.535	0.338	0.295	0.455	0.113	1.777	2.249	2.364	1.512	0.748
Ca	1.172	0.977	0.627	0.501	0.247	0.493	0.121	1.303	1.217	1.170	0.346	0.021
Na	1.532	1.468	1.841	1.904	2.175	1.801	2.551	0.925	1.468	1.464	2.224	2.032
K	0.206	0.230	0.234	0.360	0.438	0.379	0.350	0.213	0.235	0.257	0.291	0.333

Fe₂O₃ determined after the method of Leake (1978)

of more evolved pyroxenes from isolated patches of liquid with varying minor element chemistry. Mn contents reflect the availability of suitable structural sites in the evolving pyroxenes, and in this way reflect the behaviour of Fe^{2+} . With increasing aegirite content there is a pronounced decrease of Mn in the pyroxenes. The Mulanje pyroxenes, with the exception of the nearly pure aegirines, show a uniformly low content of Al (fig. 3). Unlike the situation in many similar complexes from the Gardar Province of South-West Greenland (see Stephenson and Upton, 1982), there is no pronounced enrichment of Al in the less evolved, more diopside-rich pyroxenes. However, Al contents very similar to those presented here have been observed in pyroxenes from the silica-oversaturated syenitic and granitic rocks of the Kangerdlugssuaq Intrusion of East Greenland (Brooks and Gill, 1982). The lack of Al-enrichment in early pyroxenes

is perhaps more typical of silica-oversaturated than of silica-undersaturated syenite complexes.

Amphiboles. Selected amphibole analyses are given in Table II. The complete range of amphibole compositions is shown in fig. 4 in terms of $(Al^{IV} + Ca)$ and $(Si + Na + K)$ (Giret *et al.*, 1980). Compositional ranges and the direction of change, as indicated by textural evidence, within individual rocks are represented by arrows. As is seen from fig. 5, the amphiboles of the Main complex are decidedly more iron-rich than those from Chambe and the richteritic amphiboles of the Main complex (fig. 4) should more correctly be termed ferrichterites (i.e. $Mg/(Mg + Fe^{2+} + Mn) < 0.5$).

The general evolutionary trend of the Main complex amphiboles is kataphorite \rightarrow ferrichterite \rightarrow arfvedsonite (fig. 4) which essentially correlates with a change in rock type from syenite to granite. Superimposed on the Main complex trend

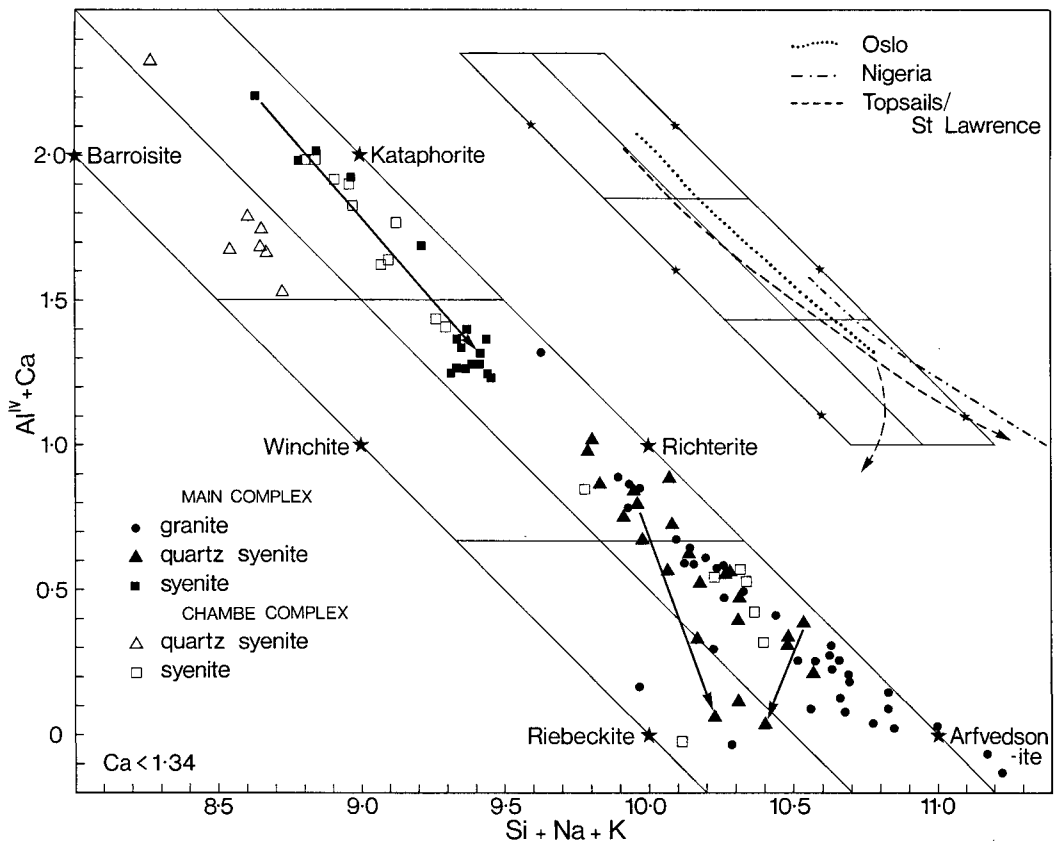


Fig. 4. Plot of Mulanje amphiboles in terms of $(Al^{IV} + Ca)$ against $(Si + Na + K)$. Solid symbols, Main complex; open symbols, Chambe complex. The key indicates the nature of the host rock. Arrows indicate variation and direction, from textural evidence, of amphibole compositions. Trends for three similar areas are indicated on the inset diagram (after Strong and Taylor, 1984, fig. 6A and B, and Giret *et al.*, 1980, fig. 2).

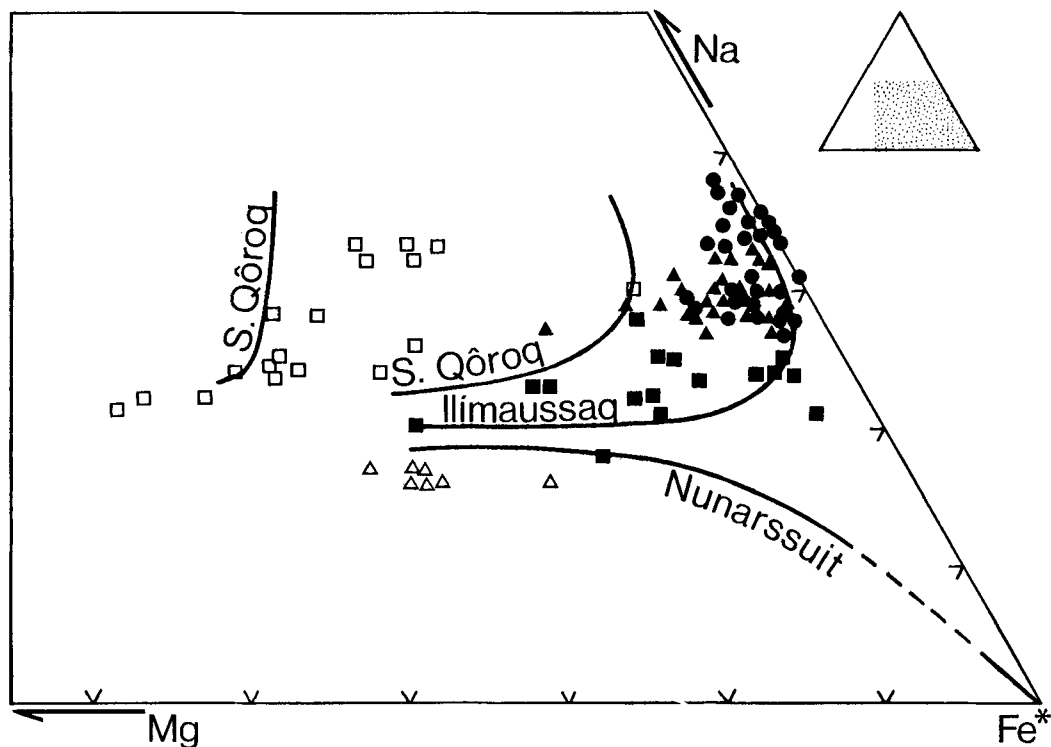


FIG. 5. Plot of amphiboles in part of the system Mg-Fe-Na (Fe^* = total iron as Fe^{2+}) (atoms). Symbols as for fig. 4. For comparison, trends for Nunarssuit, Ilímaussaq and S. Qôroq are also shown (after Stephenson and Upton, 1982, fig. 5).

is a similar, yet less extensive trend of the more Mg-rich Chambe amphiboles (fig. 4). These two trends (figs. 4 and 5) broadly mimic the compositional trends of the Chambe and Main complex pyroxenes (fig. 2).

The general trend for magmatic amphiboles from the Mulanje Massif corresponds well to the general trend of amphibole evolution in peralkaline silica-oversaturated rocks illustrated by Giret *et al.* (1980, fig. 5). Similar trends from silica-saturated and oversaturated complexes reported by Strong and Taylor (1984, fig. 6) are illustrated in fig. 4 (inset). In relation to these complexes, the range of amphibole compositions from the Mulanje Massif is exceptionally extensive. Strong and Taylor (1984) have defined this principal trend from kataphorite to arfvedsonite as the 'magmatic/subsolidus trend'.

Riebeckitic amphibole replaces ferrorichterite and arfvedsonite, and occurs as small acicular grains along veinlets and on the surface of larger crystals in the quartz syenites and granites of the Main complex. This suggests secondary development of riebeckite and correlates well with the

subsidiary trend of Giret *et al.* (1980) and the oxidation trend of Strong and Taylor (1984). The latter authors consider this trend to be hydrothermal in origin and we agree with this.

The small group of barroisitic amphiboles (figs. 4 and 5) which lie away from the main trend are somewhat unusual. They are, however, recorded from a single Chambe quartz syenite which contains dolerite inclusions; contamination of the magma from which they crystallized is therefore a distinct possibility.

Micas. Selected mica analyses are given in Table III and compositions in terms of Mg-Fe-Al are plotted in fig. 6. Again, as with the pyroxenes and amphiboles, the Chambe complex micas are more Mg-rich than those from the Main complex (fig. 6). Micas from both complexes show a general evolution to more iron-rich compositions, with relatively constant Al content.

Micas from the Main Complex show extreme iron enrichment with $\text{Mg}/(\text{Mg} + \text{Fe}^{2+})$ ratios (*total iron calculated as Fe^{2+}) of 0.005-0.14. Ferric iron determinations by Dr A. J. Easton of

a carefully handpicked mica with a very low $Mg/(Mg + Fe^{2+})$ ratio (< 0.02) failed to show the presence of this ion. This is perhaps a little surprising as Hazen and Wones (1972) have predicted that most reduced synthetic annites will have an appreciable ferric iron (oxyannite) component. However, Foster (1960, Table II) has reported a ferruginous biotite with only a trace amount of ferric iron.

TABLE III
REPRESENTATIVE ANALYSES OF MICA

Sample	Main complex		Chambe complex	
	71	96	105	100
SiO ₂	35.50	36.24	37.77	38.64
Al ₂ O ₃	7.29	8.79	10.35	9.24
TiO ₂	2.78	3.89	3.61	1.99
FeO*	38.15	33.25	19.15	27.82
MnO	0.66	0.56	0.74	1.26
MgO	0.28	3.01	12.56	7.35
CaO	0.04	0.11	0.00	0.20
Na ₂ O	0.65	0.53	0.59	0.45
K ₂ O	8.82	8.24	9.60	9.55
TOTAL	94.17	94.62	94.37	96.50
Structural formula based on 22 oxygens				
Si	6.100	6.015	58.804	6.124
Al	1.476	1.721	1.898	1.726
Ti	0.359	0.486	0.423	0.237
Fe	5.482	4.616	2.492	3.688
Mn	0.096	0.079	0.097	0.169
Mg	0.073	0.744	2.915	1.737
Ca	0.008	0.019	0.000	0.033
Na	0.215	0.171	0.179	0.137
K	1.933	1.746	1.906	1.931

*Total iron as FeO

Wones and Eugster (1965) have shown experimentally that increasing annite content of micas is a function of falling temperatures and f_{O_2} . The mica data are therefore consistent with those from the coexisting pyroxene and amphibole in that they suggest lower f_{O_2} for the Main complex magmas than in the Chambe magmas. The most extreme annite enrichment occurs in peralkaline granites of the Main complex, indicating that these formed from the most evolved and lowest temperature magmas of the Mulanje Massif.

Aenigmatite is an abundant phase in the quartz syenites and granites of the Main complex of the Mulanje Massif. It does not occur, however, in rocks from the Chambe complex. Representative analyses are given in Table IV. On the basis of 20 oxygen atoms per structural formula, the aenigmatites from Mulanje have a Si range of 5.88 to 6.07,

close to the idealized formula and similar to the range obtained from the literature (i.e. 5.8 to 6.0) for aenigmatites in silica-oversaturated peralkaline syenites and granites. Aenigmatites from silica-undersaturated rocks have Si contents between 5.3 and 5.8 presumably reflecting a lower silica activity.

Aenigmatite stability in peralkaline magmas is strongly dependent on oxygen fugacity (Nicholls and Carmichael, 1969; Marsh, 1975). The absence of aenigmatite from the peralkaline rocks of the Chambe complex, and its presence in similar rocks of the Main complex, is attributed to a higher oxygen fugacity of the Chambe magmas.

Astrophyllite is observed in some of the more highly evolved peralkaline quartz syenites and granites of the Main complex but is totally absent from the Chambe rocks. Again, this might reflect the higher oxygen fugacities of the Chambe magmas. Where particularly abundant, it is found in association with annite and sodic amphibole but never with ilmenite or aenigmatite. Analyses of two such astrophyllites are given in Table IV, from which it is seen that they contain significant amounts of Nb and Zr.

In certain quartz syenites and granites, astrophyllite has been observed partially replacing aenigmatite in what might be considered a metastable relationship. This is supported by Marsh (1975) who considers that astrophyllite and aenigmatite have different temperatures of stability. He suggests that astrophyllite should be considered the low-temperature hydrated equivalent of aenigmatite. Certainly this conjecture is supported by the mineralogy of the more evolved, lower temperature peralkaline granites of the Mulanje Massif.

Fayalite. The olivine (fayalite) of the Main complex rocks is generally highly altered. It is in general only observed in the less evolved syenites of this complex. A single analysis of fayalite has been obtained and is presented in Table IV.

Opaque oxides are minor phases in the rocks of the Mulanje Massif, with discrete ilmenite occurring in rocks of both complexes and exsolution pairs of magnetite and ilmenite restricted to the Chambe complex.

The discrete ilmenite grains show considerable, if somewhat variable, manganese substitution for iron. The measure of this substitution is illustrated in fig. 7 in which tie lines indicate the range of compositions found within individual rocks. In general, the Chambe ilmenites are slightly richer in Mn than those of the Main complex. Within both rock series there is, however, no convincing correlation of Mn content with the degree of evolution of the rock types. This is contrary to the findings of Neumann (1974) who reported that the ratio of

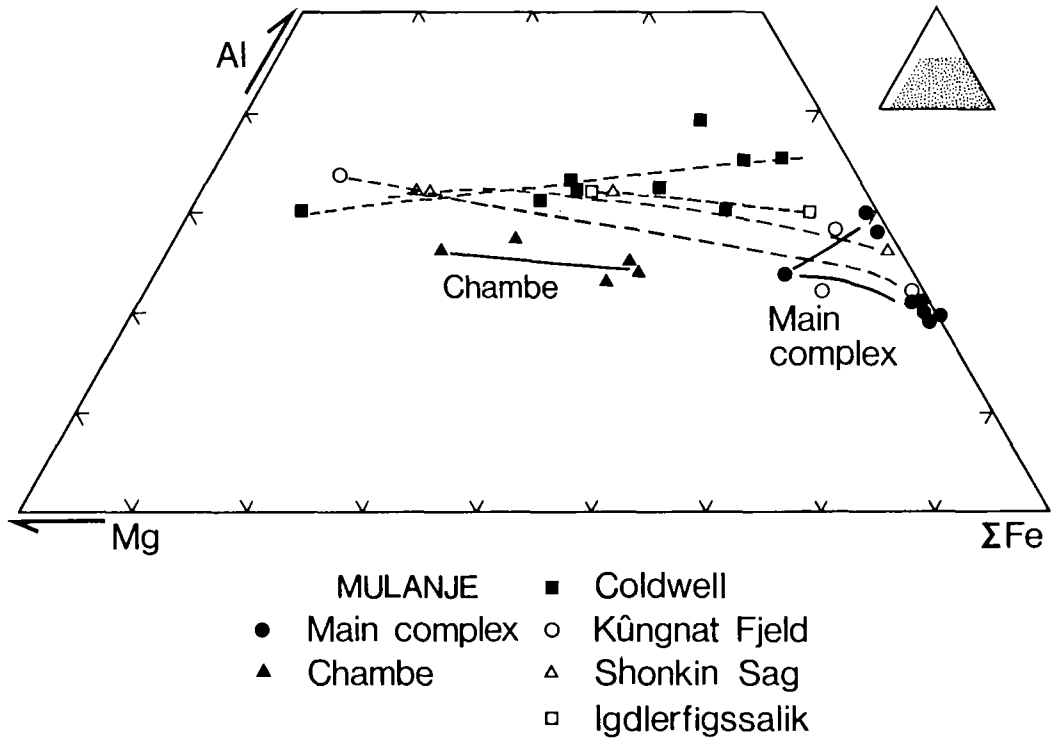


FIG. 6. Plot of micas in part of the system Mg-Fe-Al (ΣFe = total iron as Fe^{2+}). Trends for a number of other complexes are shown: see key. Sources of the data are as follows: Coldwell, Mitchell and Platt, 1982; Kûngnat Fjeld, Stephenson and Upton, 1982; Shonkin Sag, Nash and Wilkinson, 1970; Igdlarfígssalik, Powell, 1978.

Mn/Fe^{2+} in ilmenites increases with increasing differentiation index.

Moderate tenors of Nb, generally in the range of 0.4–0.5% but up to 1.6%, are also found in the discrete ilmenite grains of both complexes.

Rocks of the Chambe complex invariably contain magnetite-ilmenite exsolution pairs formed by the subsolidus unmixing of original titaniferous magnetites. Detailed studies of these have not been made.

Discussion

The Mulanje Massif is essentially similar to other felsic intrusive bodies associated with continental rift structures (e.g. the Gardar intrusions of South-West Greenland). Evidence of associated volcanic covers and intrusion by cauldron subsidence (Ofstedahl, 1978; Chapman, 1976; Mitchell and Platt, 1982) suggests that felsic intrusions of this type are intruded at relatively shallow depths under correspondingly low pressures of 1–2 kbar. Field indications of cauldron subsidence associated with

the Chambe ring structure (Stringer *et al.*, 1956) and of a now eroded volcanic suite—the Tuchila volcanics (Garson and Walshaw, 1969), both suggest a subvolcanic origin for the Mulanje Massif. Crystallization pressures of the order of 1–2 kbar, therefore, could reasonably be expected for both the Main and the Chambe complexes.

The mineral data presented in this paper for rocks of the Main complex reveal an unusually extensive and complete evolution of the pyroxene and amphibole series. However, there is little evidence of crystal accumulation that would perhaps lead to the preservation of early-formed crystal fractions, although what are interpreted as cumulate textures are preserved in some rocks. Zoning is exceptional rather than the rule in the major mafic phases, yet rather wide compositional ranges for pyroxenes and amphiboles are found within individual rocks.

The very large size of the Main complex and the apparent lack of internal contacts indicate a very slow rate of cooling, despite the high level of emplacement. The slow cooling rate would

TABLE IV
 REPRESENTATIVE ANALYSES OF
 AENIGMATITE, ASTROPHYLLITE AND FAYALITE

Sample	2	89	71	72	96	123	116
SiO ₂	41.11	41.88	34.11	34.65	35.65	34.59	29.82
Al ₂ O ₃	0.53	0.20	0.92	0.82	1.30	0.52	0.07
TiO ₂	8.89	9.13	7.16	8.65	10.45	11.92	0.06
FeO*	40.16	39.37	33.84	34.45	29.91	31.40	62.20
MnO	1.67	2.01	1.99	1.85	4.05	4.00	5.40
MgO	0.02	0.00	0.00	0.03	0.82	0.25	0.92
CaO	0.31	0.08	0.24	0.51	1.28	1.09	0.13
Na ₂ O	7.01	7.19	2.63	2.66	2.34	2.41	0.54
K ₂ O	0.02	0.11	5.93	5.66	6.01	5.72	0.03
ZrO ₂	-	-	1.88	1.50	1.12	0.10	0.00
Nb ₂ O ₅	-	-	4.88	2.98	0.57	0.40	0.11
Total	99.72	99.97	93.58	93.76	93.50	92.40	99.28

Structural formula based on:

	20 Oxygens		29 Oxygens				4 Oxygens
Si	5.928	6.000	7.946	7.975	8.062	7.978	1.005
Al	0.090	0.034	0.261	0.232	0.348	0.142	0.003
Ti	0.964	0.983	1.247	1.508	1.769	2.068	0.002
Fe	4.844	4.717	6.583	6.641	5.655	6.057	1.754
Mn	0.204	0.244	0.406	0.348	0.783	0.781	0.154
Mg	0.004	0.000	0.000	0.000	0.261	0.084	0.046
Ca	0.047	0.013	0.058	0.116	0.319	0.270	0.005
Na	1.961	1.998	1.189	1.189	1.015	1.076	0.035
K	0.000	0.019	1.769	1.653	1.740	1.684	0.001
Zr	-	-	0.203	0.174	0.116	0.012	0.000
Nb	-	-	0.522	0.319	0.058	0.041	0.002

*Total iron as FeO

Samples 2, 89 Aenigmatite; 71, 72, 96, 123 Astrophyllite; 116, Fayalite. All rocks from the Main complex.

account presumably for the lack of zoning in early-formed phases but would seem to preclude the broad compositional ranges found within individual rocks. It is suggested that these observations can be reconciled by considering that crystallization proceeded essentially in three stages.

The first stage involved a magma with a high proportion of liquid. There may have been some crystal settling with concomitant migration of residual liquid towards the roof. The mapping of Walshaw (Garson and Walshaw, 1969; 1:100 000 geological map) seems to indicate a concentration of granite in the upper parts of the Main complex, although in the southeast this is not the case, suggesting some differentiation before emplacement. Equilibration of crystals and liquid at this stage would be rapid.

The second stage would be reached when crystallization advanced enough to prevent, or inhibit, large-scale movement of residual melt. There would now effectively be an infinite number of tiny closed systems, a situation somewhat akin to the trapping of closed system liquids in compacted cumulus

piles, as proposed by Mitchell and Platt (1978). Minerals crystallizing at this stage would evolve rapidly, there would be reduced equilibration of liquid with previously formed crystals, and there would be a marked build up in incompatible elements and volatiles in the residual melt. This would lead to the third stage characterized essentially by subsolidus growth promoted by residual fluids migrating along grain boundaries and perhaps hydraulic fractures.

Crystallization of the main pyroxene and amphibole trends seems to be confined to the first two stages. Mica, astrophyllite, and chevkinite occur late in the second stage, while unidentified rare earth minerals, yttrifluorite and riebeckite crystallize during the third stage only. Such a model is consistent with the textures of the rocks and conforms well with the overall evolution of the mafic minerals.

General indications of f_{O_2} and accompanying crystallization temperatures of the Main complex magmas are obtained from the crystallizing mafic minerals. The progressive alkali enrichment and peralkaline nature of the Main complex magmas

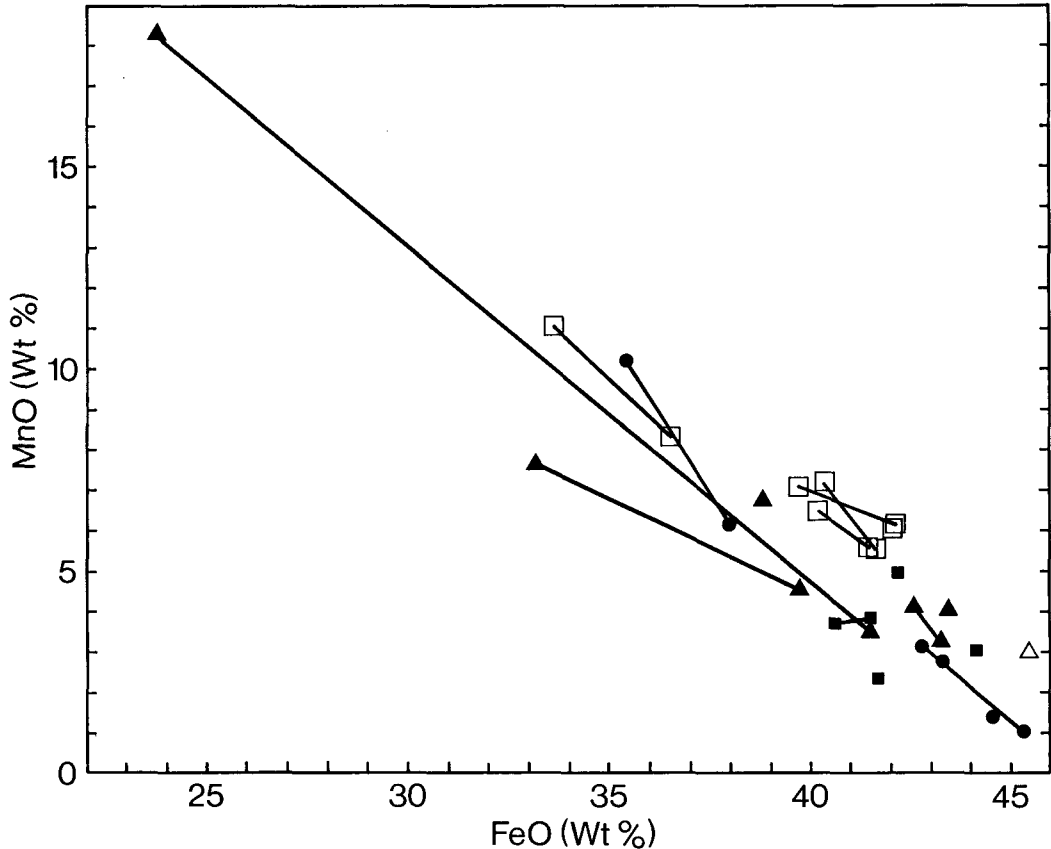


Fig. 7. Plot of FeO against MnO [wt. %] for ilmenites. Tie-lines indicate range of compositions within individual rocks. Symbols as on fig. 4.

during stages 1 and 2 is reflected in the compositional trends of the pyroxenes (fig. 2) and the amphiboles (fig. 4). The presence of aenigmatite and late-forming astrophyllite provide additional evidence for this general evolution.

Piotrowski and Edgar (1970) and Sood and Edgar (1970) have established experimentally that peralkaline felsic magmas have a considerable temperature interval of crystallization (i.e. 900° to 580°C), and, in consequence, a considerable range of liquidus conditions might well be expected for the Main complex magmas. In support of this, Mitchell and Platt (1978) have proposed a crystallization interval of 800/900°C to 500/550°C for the ferroaugite syenites of the Coldwell complex of Canada. Likewise, Larsen (1976) proposed an initial crystallization temperature of 800–900°C for the fayalite-augite syenites from the Ilímaussaq complex, Greenland.

Variations in f_{O_2} for the Main complex magmas,

during stages 1 and 2, should be considered for a crystallization interval not unlike those determined experimentally and by mineralogical analysis of similar rock types. The early syenites of stage 1 contain fayalite and quartz and consequently crystallize at oxygen fugacities below those defined by the quartz-fayalite-magnetite (QFM) buffer (Wones and Gilbert, 1969). Assuming initial liquidus temperatures of 800–900°C, the maximum f_{O_2} defined by the QFM buffer is $10^{-12.9}$ bars at 900°C and 10^{-15} bars at 800°C for these magmas. It is not possible to define the value more precisely. However, as a comparison, Mitchell and Platt (1978 and 1982) estimated f_{O_2} values of 10^{-15} bars and 10^{-14} bars respectively for early crystallizing ferro-augite syenites and nepheline syenites of the Coldwell complex.

With evolution, the Main complex magmas became increasingly peralkaline and this peralkalinity is well established by stage 2. Fayalite even-

tually becomes unstable in response to increasing magma peralkalinity with the most likely reaction leading to the production of acmite, as in the equation quoted earlier (p. 90).

The acmite molecule so produced enters the pyroxene solid solution, which is already becoming increasingly rich in this component with the increasing peralkalinity of the magmas. Uncertainties in free energy values of acmite make f_{O_2} values associated with the above reactions uncertain. Using the free energy data of Nicholls and Carmichael (1969), however, f_{O_2} estimates for a temperature range of 600–700°C are 10^{-21} to 10^{-18} bars respectively.

These values might not be unreasonable in the light of the presence of ferrichteritic amphiboles in the more evolved quartz-bearing syenites and quartz syenites of the Main complex (fig. 4). Over a similar temperature range, Charles (1975) established maximum f_{O_2} values for the stability of ferrichterite of 10^{-22} bars to 10^{-19} bars, respectively.

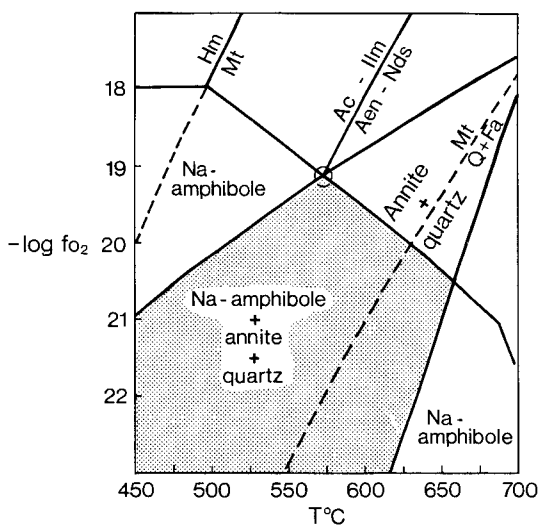
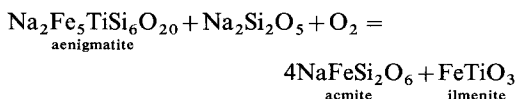


FIG. 8. Oxygen fugacity temperature diagram for conditions of late-stage liquids of the Main complex. See text for explanation.

The most evolved peralkaline granites of stage 2 characteristically have the assemblage quartz + annite + arfvedsonite (Na-amphibole). The T - f_{O_2} stability of this assemblage (Ernst, 1962, and Eugster and Wones, 1962) is shown as the shaded area in fig. 8, and it can be expected that the residual granites crystallized within this general field.

The point of intersection between the above field and the reaction curve after Nicholls and Carmichael (1969) of:



occurs at approximately 570°C and 10^{-19} bars f_{O_2} . This intersection is of interest as granites have been identified with the assemblage arfvedsonite + annite + acmite + aenigmatite + ilmenite + quartz. Such an assemblage might represent non-equilibrium conditions but its preservation far removed from the T - f_{O_2} conditions of the intersection point would not be expected. Imprecise knowledge of the free energies of aenigmatite and arfvedsonite unfortunately prevent the exact parameters of the intersection point from being established at present. The values of 570°C and 10^{-19} bars are therefore, at best, approximations. However if, as established from mineralogical studies of similar intrusions and from experimental work, the crystallization temperatures of the Main complex magmas are of the order of 900–550°C, then a concomitant range of f_{O_2} of 10^{-13} to 10^{-20} bars respectively might reasonably be expected for them.

Subsolidus stage 3 crystallization in the Main complex rocks resulted in the formation of mica, riebeckite, yttrifluorite, a variety of as yet unidentified rare-earth-rich minerals, and small cross-cutting veins of albite. This assemblage is considered to have formed in response to the action of moderately hot alkali and rare-earth-enriched residual fluids. Ernst's (1962) study of riebeckite stability suggests that the maximum temperature of these liquids is 496 ± 5 °C with a corresponding f_{O_2} defined by the hematite-magnetite buffer.

The rocks of the Chambe complex, although showing broad mineralogical similarities, are distinct from those of the Main complex. They are poorer in quartz and consist essentially of slightly silica-oversaturated syenites and minor quartz syenites; granites do not occur. This more restricted range of rock types is reflected by the smaller ranges of pyroxene and amphibole compositions (figs. 2 and 4). Moreover, compositions of both these mineral groups are consistently more magnesian than those of the Main complex. As discussed previously in this paper, these compositional differences might be explained by crystallization under higher f_{O_2} conditions or the earlier development of peralkaline tendencies in the Chambe magmas or both. The higher f_{O_2} values of the Chambe magmas, when compared with those of the Main complex, is evident from the presence of magnetite and the absence of fayalite in

quartz-bearing assemblages. These magmas have consequently crystallized at oxygen fugacities above those defined by the QFM buffer (Wones and Gilbert, 1969).

These higher oxygen fugacities also explain the absence of the typical peralkaline indicator mineral aenigmatite, despite evidence from the pyroxenes and amphiboles that the Chambe magmas became peralkaline with evolution. At higher f_{O_2} aenigmatite becomes unstable and produces acmite and ilmenite by the reaction cited earlier (p. 97).

As discussed previously, an earlier development of peralkaline tendencies acting in conjunction with higher f_{O_2} can explain the evolutionary trends of the Chambe pyroxenes and amphiboles. If the parental Chambe magmas had a lower silica activity and a lower alkali/alumina ratio than those of the Main complex, they would have had a smaller crystallization interval and thus less chance to generate late, residual peralkaline granitic liquids. It is in this type of liquid that the most evolved pyroxenes and amphiboles are encountered in the Main complex.

We suggest, therefore, that the Chambe complex was formed by the intrusion of a slightly silica-oversaturated parental magma. Evolution of this magma under moderately high f_{O_2} (i.e. above the QFM buffer) eventually produced peralkaline quartz-bearing syenites and quartz syenites. However, the original magma composition and limited crystallization interval prevented the formation of late-stage peralkaline granites so evident in the Main complex.

Acknowledgements. The authors would like to express their appreciation to the Government of Malawi for permission to conduct the necessary field work in the Mulanje region and to the Malawi Geological Survey for providing logistical support. The manuscript has greatly benefited from the critical readings of Drs A. C. Bishop, D. R. C. Kempe, and R. H. Mitchell. We also wish to thank Miss V. Jones for drafting the figures and Dr A. J. Easton for determining the ferric iron content of a biotite sample. R. G. Platt also acknowledges support for this project from NSERC operating grant A9169.

REFERENCES

- Brooks, C. K., and Gill, R. C. O. (1982) Compositional variation in the pyroxenes and amphiboles of the Kangerdlugssuaq intrusion, East Greenland: further evidence for the crustal contamination of syenite magma. *Mineral. Mag.* **45**, 1-9.
- Carmichael, I. S. E., and Nicholls, J. (1967) Iron-titanium oxides and oxygen fugacities in volcanic rocks. *J. Geophys. Res.* **72**, 4665-87.
- Chapman, C. A. (1976) Structural evolution of the White Mountain Magma Series. *Geol. Soc. Am. Mem.* **146**, 281-300.
- Charles, R. W. (1975) The phase equilibria of richterite and ferrichterite. *Am. Mineral.* **60**, 367-74.
- Ernst, W. G. (1962) Synthesis, stability relations, and occurrence of riebeckite and riebeckite-arfvedsonite solid solutions. *J. Geol.* **70**, 689-736.
- Eugster, H. P., and Wones, D. R. (1962) Stability relations of the ferruginous biotite annite. *J. Petrol.* **3**, 82-125.
- Foster, M. D. (1960) Interpretation of the composition of trioctahedral micas. *U.S. Geol. Surv. Prof. Paper* **354-B**, 1-49.
- Fudali, R. F. (1965) Oxygen fugacities of basaltic and andesitic magmas. *Geochim. Cosmochim. Acta*, **29**, 1063-75.
- Garson, M. S., and Walshaw, R. D. (1969) The geology of the Mlanje area. *Geol. Surv. of Malawi Bull.* **21**, 1-157.
- Giret, A., Bonin, B., and Leger, J.-M. (1980) Amphibole compositional trends in oversaturated alkaline plutonic ring-complexes. *Can. Mineral.* **18**, 481-95.
- Hazen, R. M., and Wones, D. R. (1972) The effect of cation substitutions on the physical properties of trioctahedral micas. *Am. Mineral.* **57**, 103-29.
- Larsen, L. M. (1976) Clinopyroxenes and coexisting mafic minerals from the alkaline Ilmaussaq intrusion, South Greenland. *J. Petrol.* **17**, 258-90.
- Leake, B. E. (1978) Nomenclature of amphiboles. *Mineral. Mag.* **42**, 533-63.
- Marsh, J. S. (1975) Aenigmatite stability in silica-undersaturated rocks. *Contrib. Mineral. Petrol.* **50**, 135-44.
- Mitchell, R. H., and Platt, R. G. (1978) Mafic mineralogy of ferroaugite syenite from the Coldwell alkaline complex, Ontario, Canada. *J. Petrol.* **19**, 627-51.
- (1982) Mineralogy and petrology of nepheline syenites from the Coldwell alkaline complex, Ontario, Canada. *Ibid.* **23**, 186-214.
- Nash, W. P., and Wilkinson, J. F. G. (1970) Shonkin Sag laccolith, Montana. I. Mafic minerals and estimates of temperature, pressure, oxygen fugacity and silica activity. *Contrib. Mineral. Petrol.* **25**, 241-69.
- Neumann, E.-R. (1974) The distribution of Mn^{2+} and Fe^{2+} between ilmenites and magnetites in igneous rocks. *Am. J. Sci.* **274**, 1074-88.
- (1976) Compositional relations among pyroxenes, amphiboles and other mafic phases in the Oslo Region plutonic rocks. *Lithos*, **9**, 85-109.
- Nicholls, J., and Carmichael, I. S. E. (1969) Peralkaline acid liquids: a petrological study. *Contrib. Mineral. Petrol.* **20**, 268-94.
- Oftedahl, C. (1978) Main geologic features of the Oslo Graben. In I. B. Ramberg and E.-R. Neumann (eds.) *Tectonics and Geophysics of continental rifts*. 149-65. Riedel, Dordrecht.
- Paul, A., and Douglas, R. W. (1965) Ferrous-ferric equilibrium in binary alkali silicate glasses. *Physics and Chemistry of Glasses*, **6**, 207-11.
- Piotrowski, J. M., and Edgar, A. D. (1970) Melting relations in undersaturated alkaline rocks from Greenland, Africa and Canada. *Meddelelser om Grønland*, **181**, Nr. 9.
- Powell, M. (1978) The crystallisation history of the Igdlarfigssalik nepheline syenite intrusion, Greenland. *Lithos*, **11**, 99-120.

- Sood, M. K., and Edgar, A. D. (1970) Melting relations of undersaturated alkaline rocks from the Ilimaussaq intrusion and Gronnedal-Ika complex South Greenland, under water vapour and controlled partial oxygen pressure. *Meddelelser om Grønland*, **81**, Nr. 12.
- Stephenson, D. (1972) Alkali clinopyroxenes from nepheline syenites of the South Qoroq Centre, south Greenland. *Lithos*, **5**, 187-201.
- and Upton, B. G. J. (1982) Ferromagnesian silicates in a differentiated alkaline complex: Kūngnāt Fjeld, South Greenland. *Mineral. Mag.* **46**, 283-300.
- Stringer, K. V., Holt, D. N., and Groves, A. W. (1956) The Chambe Plateau ring complex of Nyasaland. *Colonial Geology and Mineral Resources*, **6**, 3-18.
- Strong, D. F., and Taylor, R. P. (1984) Magmatic-subsolidus and oxidation trends in composition of amphiboles from silica-saturated peralkaline igneous rocks. *Tschermks Mineral. Petrog. Mitt.* **32**, 211-22.
- Tyler, R. C., and King, B. C. (1967) The pyroxenes of the alkaline igneous complexes of eastern Uganda. *Mineral. Mag.* **36**, 5-21.
- Wones, D. R., and Eugster, H. P. (1965) Stability of biotite: experiment, theory, and application. *Am. Mineral.* **50**, 1228-72.
- and Gilbert, M. C. (1969) The fayalite-magnetite-quartz assemblage between 600° and 800 °C. *Am. J. Sci.* **267-A**, 480-8.
- Woolley, A. R., and Garson, M. S. (1970) Petrochemical and tectonic relationship of the Malawi carbonatite-alkaline province and the Lupata-Lebombo volcanics. In T. N. Clifford and I. G. Gass (eds.), *African Magmatism and Tectonics*, 237-62. Oliver and Boyd, Edinburgh.
- Yagi, K. (1953) Petrochemical studies of the alkalic rocks of the Morotu district, Sakhalin. *Bull. Geol. Soc. Am.* **64**, 769-810.

[Manuscript received 8 February 1985]